On the Universal Scaling Behavior of the Distance Decay of Plasmon Coupling in Metal Nanoparticle Pairs: A Plasmon Ruler Equation

Prashant K. Jain,[†] Wenyu Huang,[†] and Mostafa A. El-Sayed*,[†,‡]

Laser Dynamics Laboratory, School of Chemistry and Biochemistry, Georgia Institute of Technology, Atlanta, Georgia 30332-0400, University of California, Berkeley, California 94720

Received April 27, 2007; Revised Manuscript Received May 23, 2007

ABSTRACT

Localized surface plasmon resonances (LSPR) in lithographically fabricated gold (Au) nanodisc pairs are investigated using microabsorption spectroscopy and electrodynamic simulations. In agreement with previous work, we find that the fractional plasmon wavelength shift for polarization along the interparticle axis decays nearly exponentially with the interparticle gap. In addition, we find that the decay length is roughly about 0.2 in units of the particle size for different nanoparticle size, shape, metal type, or medium dielectric constant. The near-exponential distance decay and the interesting "universal" scaling behavior of interparticle plasmon coupling can be qualitatively explained on the basis of a dipolar-coupling model as being due to the interplay of two factors: the direct dependence of the single-particle polarizability on the cubic power of the particle dimension and the decay of the plasmonic near-field as the cubic power of the inverse distance. Using this universal scaling behavior, we are able to derive a "plasmon ruler equation" that estimates the interparticle separation between Au nanospheres in a biological system from the observed fractional shift of the plasmon band. We find good agreement of the interparticle separations estimated using this equation with the experimental observations of Reinhard et al. (*Nano Lett.* 2005, 5, 2246–2252).

The unique interaction of metal nanoparticles with electromagnetic radiation is constituted by localized surface plasmons, which are coherent oscillations of the metal electrons in resonance with light of a certain frequency, i.e., the localized surface plasmon resonance (LSPR) frequency.[1–6] The LSPR results in a strongly enhanced electric *near-field* localized at the particle surface, which forms the basis of surface-enhanced spectroscopy using metal nanoparticles.[7,8] The plasmon oscillations also decay radiatively or nonradiatively, respectively, giving rise to strongly enhanced scattering (in the *far-field*) and absorption at the LSPR frequency.[2,9,10] These optical properties have been utilized in optical technologies for chemical and biological imaging,[11,12] sensing,[13–15] and therapeutics.[16–19] Many of the applications of metal nanoparticles are being realized from their assemblies and hence, recent studies have been focused on the assemblies/arrays of metal nanoparticles.[20] These studies have established that the plasmonic properties are strongly dependent on interparticle interactions.[21–29] The *near-field* on one particle has the ability to interact with that on an adjacent particle in close proximity, coupling the

plasmon oscillations together.[1,23,28,30,31] This interparticle plasmon coupling forms the basis of the intense enhancement of spectroscopic signals (e.g., SERS) from molecules adsorbed at nanoparticle junctions, providing the capability for single-molecule sensing and detection.[32,33] Near-field coupling in ordered nanoparticle assemblies has also been exploited for electromagnetic energy transport and subwavelength photonic waveguiding.[34–37]

The coupled-particle LSPR occurs at a frequency that is shifted from the single-particle LSPR frequency. The assembly or aggregation of gold nanoparticles in solution results in a red-shift of the plasmon extinction wavelength maximum from that of isolated gold nanoparticle solution at ~520 nm, as also evidenced by a visual color change from red to purple.[22,38,39] As shown by the Alivisatos and Mirkin groups,[40,41] by employing a biomolecular recognition event (e.g., DNA hybridization) to trigger the assembly of nanoparticles in solution, the spectral shift in the plasmon resonance can be employed to detect specific biomolecules including DNA and protein biomarkers for cancer and other diseases.[13]

The magnitude of the assembly-induced plasmon shift depends on the strength of the interparticle coupling, which, in turn, depends on the proximity of the individual nanoparticles. The plasmon shift thus gives a measure of the

* Corresponding author. E-mail: melsayed@gatech.edu. Telephone: 404-894-0292. Fax: 404-894-0294.
† Georgia Institute of Technology.
‡ Miller Visiting Professor, University of California, Berkeley, California 94720.

distance between the particles.[39,42,43] Sonnichsen et al. and Reinhard et al. utilized this recently to design a "plasmon ruler" to measure nanoscale distances in biological systems on the basis of the spectral shift resulting from the coupling of two gold nanoparticles by a defined biomolecular binding scheme.[42,44] The plasmon ruler has some distinct advantages over the fluorescence resonance energy transfer (FRET) technique traditionally used for distance measurement, viz. a longer distance range and better photostability of the optical probes.[42,43] However, a major prerequisite for the application of the plasmonic ruler is the systematic calibration and standardization of the spectral shift as a function of the interparticle separation.[43] While the distance dependence of FRET is well established,[45] there have been few quantitative studies on the distance dependence of plasmon coupling.[21,23,27,43] The decay of electromagnetic fields in nanostructures is also fundamentally interesting from the point of view of plasmonics.[30,34]

The electron beam lithography technique, which provides the ability to produce metal nanoparticle structures with controlled dimensions and spacing, has already been shown by Aussenegg and Krenn to be extremely powerful for such studies.[23,46−48] Recently, Su et al. studied plasmon coupling in lithographically produced elliptical gold nanoparticle pairs and observed that the plasmon shift decays almost exponentially as a function of the interparticle separation.[21] Gunnarsson et al.[27] further verified this near-exponential behavior in a system of Ag nanodisc pairs. A fundamental model explaining the distance dependence of plasmon coupling is lacking, however, which is the goal of the present work. Here, we study the plasmon resonances of lithographically fabricated pairs of Au nanodiscs for different interparticle separations. The polarization dependence of the plasmon coupling is clearly evident, in line with an earlier study by Rechberger et al.[23] The exponential-like decay of the plasmonic shift with interparticle gap for polarization along the interparticle axis is also observed. Discrete dipole approximation simulations of the nanodisc pairs verify the observation of Su et al. that the near-exponential trend of the plasmon shift with respect to the interparticle gap becomes independent of the nanodisc diameter when the shift and separation gap are scaled respectively by the single-particle plasmon wavelength and the nanodisc diameter.[21] We further find that the decay constant measured for our Au-based system matches very well with that of the Ag system studied earlier.[27] The decay constant is calculated also to be similar for nanoparticles of different shape as well as for different dielectric media. Thus, the distance decay of interparticle plasmon coupling manifests a universal scaling behavior, the origin of which we explain on the basis of a simple dipolar-coupling model.

Au Nanodisc Array Fabrication. Au nanodisc pairs were fabricated using electron beam lithography (EBL). Quartz slides (Technical Glass Products, Inc.) cleaned in piranha solution (1 part 30% H_2O_2 and 3 parts H_2SO_4) for 1.5 h at 80 °C and dried in air were spin-coated with 65 nm PMMA 950k electron-sensitive resist followed by curing at 180 °C for 3 min. In order to render the substrate conductive, it was coated with a 10 nm gold layer in a thermal evaporator. The pattern for the nanodisc array was written on the substrate using the JEOL JBX-9300FS EBL system. The gold layer was then etched with an aqueous solution of KI and I_2 followed by development in 1:3 methyl isobutyl ketone/ isopropyl alcohol for 180 s. The patterned substrate was then washed in isopropyl alcohol for 30 s and dried in pure N_2. A thin 0.4 nm Cr layer was deposited on the substrate in an electron beam evaporator in order to improve the adhesion of the subsequent Au layer deposited to a 25 nm thickness at a rate of 0.5 Å/s. Finally, the PMMA resist and the overlaying Au layer is removed by lift-off in hot acetone (∼63 °C). Following this procedure, we fabricated two-dimensional 80 μm × 80 μm arrays of 88 nm diameter Au nanodiscs with an interparticle center-to-center spacing of 300 nm between the particle rows and a center-to-center spacing of 600 nm between particles within each row. In each subsequent sample, every second particle row is shifted closer to the previous row to give different arrays of particle pairs with interparticle edge-to-edge separation gap varying as 212, 27, 17, 12, 7, and 2 nm. The patterns were imaged by scanning electron microscopy (SEM) on a LEO 1530 thermally-assisted field emission SEM, Zeiss/LEO. A representative image of the array with an interparticle gap of 12 nm is shown in Figure 1. Optical spectra of the nanodisc pairs were obtained on the substrate using a SEE 1100 microabsorption spectrophotometer in the transmission mode under polarized light excitation using a 20× objective. The area examined was 8 × 8 μm^2.

Polarized Microabsorption. LSPR spectra of lithographically fabricated Au nanodisc pair arrays with different internanodisc separation gap s = 212, 27, 17, 12, 7, and 2 nm were obtained by microabsorption spectroscopy (Figure 2a,c). Two different polarization directions of the incident light were chosen, i.e., one parallel to the interparticle axis (Figure 2a) and the other perpendicular (Figure 2c) to the axis. The spectral behavior is in sharp contrast for the two polarization directions, as already observed by Tamaru et al.,[49] Rechberger et al.,[23] and Maier et al.[30] Under parallel polarization, the plasmon resonance strongly red-shifts as the interparticle gap is reduced. Conversely, there is a very weak blue-shift with decreasing gap for orthogonal polarization. The resonance shift results from the electromagnetic coupling of the single-particle plasmons, the polarization dependence of which can be explained on the basis of a simple dipole−dipole coupling model. The dipole−dipole interaction is attractive for parallel polarization, which results in the reduction of the plasmon frequency (red-shift of the plasmon band), while that for the orthogonal polarization is repulsive, resulting in the increase in the plasmon frequency (blue-shift).[23,50] The interparticle interactions are clearly stronger for parallel polarization, as seen from the larger wavelength shifts. In fact, under parallel polarization, at extremely small interparticle gaps, i.e., s = 2 nm, a new shoulder appears at shorter wavelengths, similar to earlier studies on pairs of Ag nanodisc[27] and Au nanorods[50] with nearly touching particles. It must be noted that this new band is attributed to higher-order interactions, possibly the quad-
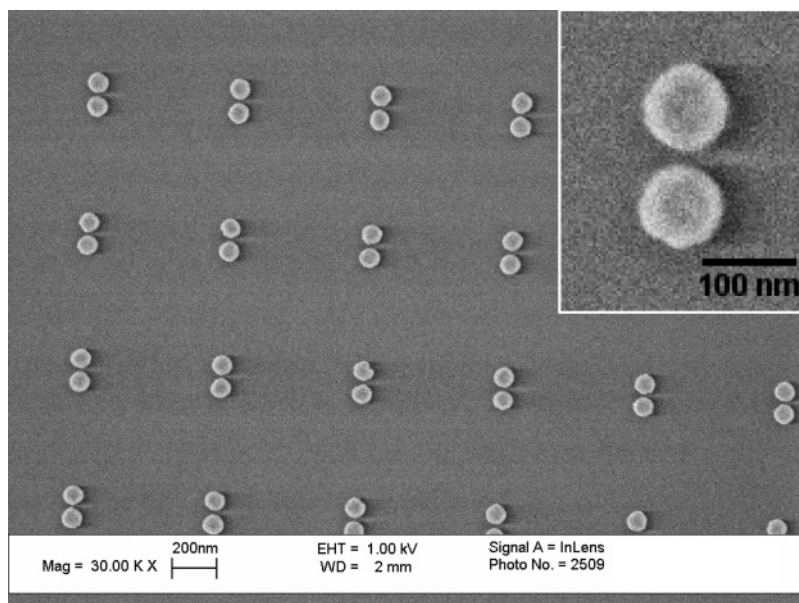
Figure 1. Representative SEM image of the array of nanodisc pairs used in the present study, having an interparticle edge-to-edge separation gap of 12 nm, showing the homogeneity of the sample. The inset shows a magnified image of a single nanodisc pair clearly showing the interparticle gap. Each nanodisc has a diameter of 88 nm and thickness of 25 nm. Images of arrays with other interparticle gaps are not shown.
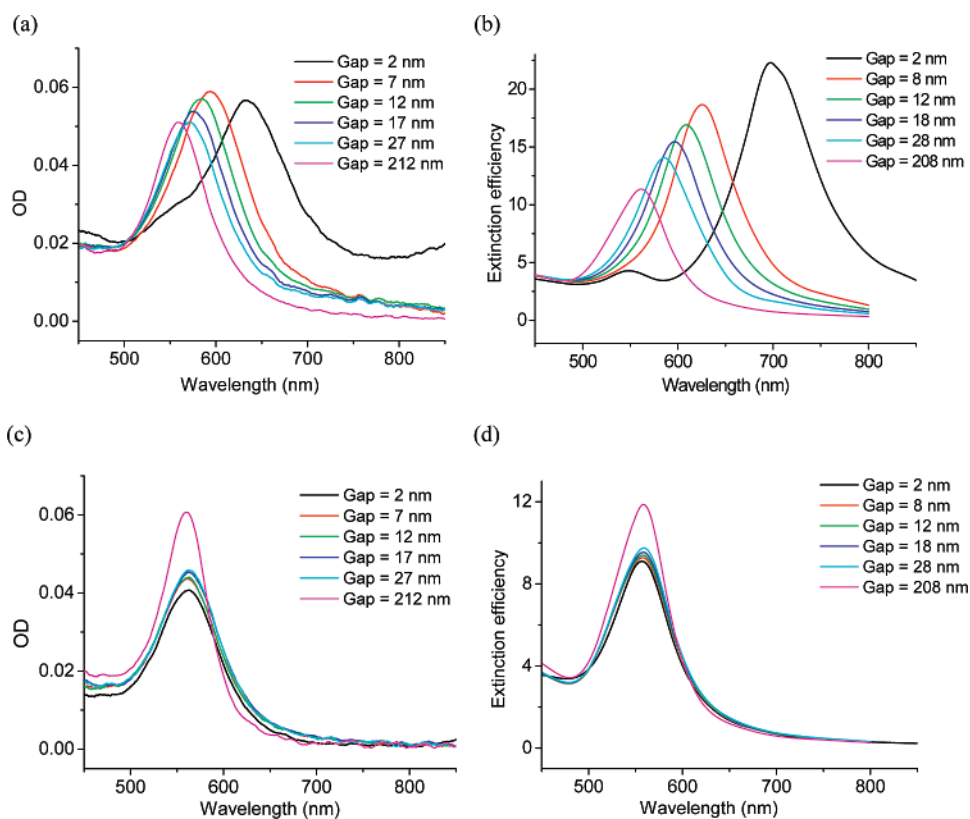

Figure 2. (a,c) Microabsorption and (b,d) DDA-simulated extinction efficiency spectra of Au nanodisc pairs for varying interparticle separation gap for incident light polarization direction (a,b) parallel and (c,d) perpendicular to the interparticle axis.

rupole mode,[27,51] and cannot be explained by the dipolar interaction model.

The shift in the plasmon extinction maximum is plotted against the interparticle edge-to-edge separation gap for the parallel polarization in Figure 3a. Note that the plasmon maximum for $s = 212$ nm (particles spaced enough to assume

minimal coupling) has been used as the reference for calculation of the shift. Because these spectra are from an ensemble of particle pairs rather than single particle pairs, the data point for $s = 2$ nm was not included due to the significant dispersion in the lithographic fabrication of such a small gap. The plot of the plasmon shift versus the
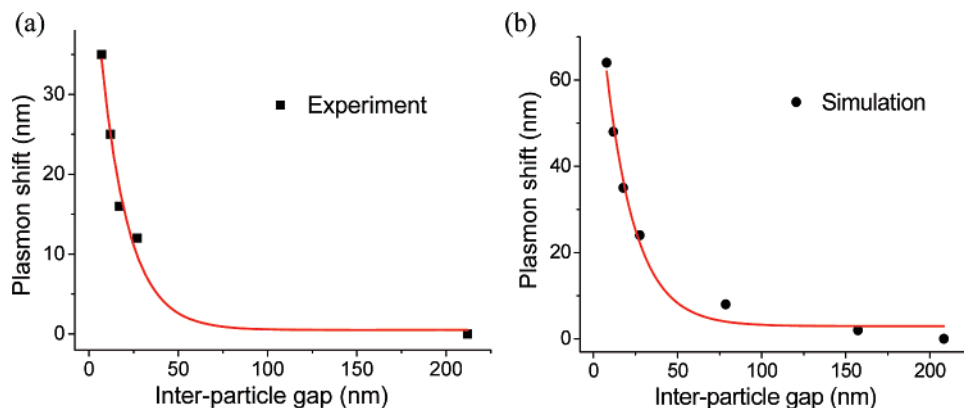
Figure 3. Shift in the plasmon wavelength maximum of a pair of Au nanodiscs as a function of the interparticle edge-to-edge separation gap for (a) experiment and (b) DDA simulation. The red curves are least-squares fits to single-exponential decay $y = y_0 + a \cdot e^{-x/l}$, yielding a decay length l of 15.5 ± 3.0 nm ($R^2 = 0.985$) for experiment and 17.6 ± 2.5 nm ($R^2 = 0.989$) for simulations.

interparticle gap follows nearly an exponential decay with a decay length of 15.5 nm ± 3.0 nm.

DDA Simulations. The discrete dipole approximation (DDA) method[52] was used to simulate the LSPR spectra of the Au nanodisc pairs. The DDA method has been demonstrated by the Schatz group to be suitable for optical calculations of the extinction spectrum and the local electric field distribution in metal particles with different geometries and environments.[2,53] While DDA has limitations in calculating electromagnetic fields around particles,[54,55] we are interested in the extinction properties of the particle pairs, which are simulated quite well by DDA, as established by the work of the Schatz group, including recent calculations of lithographically prepared silver nanodisc pairs.[27] As argued earlier by Rechberger et al.,[23] it is reasonable to consider in the calculations a single particle pair instead of the entire 2-D array. This is because the individual particle pairs in the experiment, especially for the smaller gap samples, are separated from each other well enough (much larger than 2.5 particle diameters)[21] to have any significant near-field coupling between different pairs. This ensures that only the interaction with the pair partner is important.[23]

The results of discrete dipole approximation simulations of a pair of Au nanodiscs are shown for the light polarization direction parallel to the interparticle axis (Figure 2b) and that perpendicular to the axis (Figure 2d). In our calculations, each nanodisc was approximated by a cylinder of diameter 86.5 nm and height 25.5 nm, with the cylinder axis normal to the substrate. The dielectric constant of the surrounding medium ϵ_m used was 1.0 for air, however, the most accurate treatment would require the consideration of the dielectric properties of the substrate, which consists of a quartz slide covered by a very thin chromium layer. The simulation assumes idealized isotropic cylinders with homogeneous sizes and interparticle gaps, which deviates from the true experimental situation. Our calculations also do not include a parameter to account for experimental inhomogeneities. All these factors contribute to the deviations of the DDA results from the experimental spectra. Nevertheless, the features of the experimental data are clearly reproduced in our simulation. The plasmon band for the disc pair with the maximum separation, i.e., $s = 208$ nm (which is close to 2.5 particle

diameters),[21,30] closely matches the isolated nanodisc plasmon maximum (not shown) at ∼561 nm. With decreasing interparticle gap, a strong red-shift is seen for parallel polarization, along with increase in the extinction efficiency similar to the experimental observation. When the gap reaches around 2 nm, a small shoulder emerges around 550 nm similar to the experimental case. For perpendicular polarization, only a weak blue-shift of the plasmon band with decreasing gap is seen along with a decrease in the extinction efficiency.

In the case of lithographic arrays, in addition to the near-field coupling between the particles in a pair, there also exists a far-field radiative coupling between particles at large feature separations (or grating constant) on the order of the wavelength of light. This has been studied in detail by Lamprecht et al. in 150 nm diameter gold nanodisc arrays, who showed that a change in the grating constant of the array has a significant effect on the single-particle plasmon resonance wavelength and the plasmon resonance line width.[56] In our experimental samples with small interparticle gaps (2−27 nm), the near-field coupling can be expected to be much stronger than any grating effects, while in the sample with interparticle gap of 212 nm, the grating constant is 300 nm (distance between rows), which may be lower than that required for significant far-field coupling.[23] In any case, by means of the DDA simulation of single particle pairs, we can study the near-field plasmon coupling, which is the aim of the present study, without including the complicating effect of the far-field radiative coupling or grating effects.

Figure 3b shows a plot of the DDA-simulated plasmon shift versus the interparticle separation gap for the parallel polarization. The shift can be fit very nearly to an exponential decay with a decay length of 17.6 ± 2.5 nm, close to the experimental value (Figure 3a). Note that this plot does not include the data points where the discs are nearly touching, which results in the emergence of higher-order resonances.

Scaling Behavior. Su et al. have shown that the plot of the experimentally observed plasmon shift versus interparticle separation gap follows the same trend for particles of
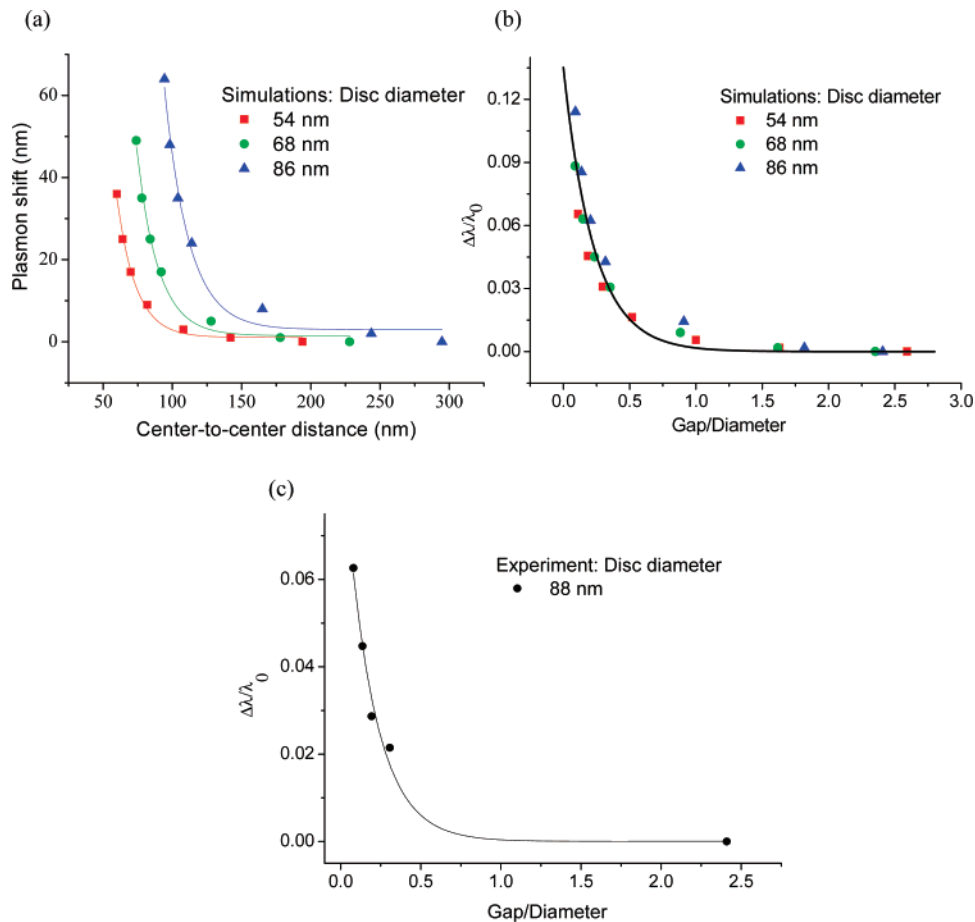
Figure 4. (a) Calculated plasmon shift vs the center-to-center distance in Au nanodisc pair for different disc diameters. The solid curves represent least-squares fits to single-exponential decay function $y = y_0 + a \cdot e^{-x/l}$. The decay lengths l obtained from the fit are 13.7, 15.5, and 17.7 nm for nanodisc diameter $D = 54$, 68, and 86 nm, respectively. (b) Calculated fractional plasmon shift vs the ratio of interparticle gap to nanodisc diameter, showing that the scaled data points for the different disc sizes follow a common trend, which can be fit together to the single-exponential decay (solid curves) $y = a \cdot e^{-x/\tau}$ with $a = 0.14 \pm 0.01$ and $\tau = 0.23 \pm 0.03$. (c) Experimental fractional plasmon shift vs ratio of gap to diameter and exponential fit (solid curve) with $a = 0.10 \pm 0.01$ and $\tau = 0.18 \pm 0.02$.

different dimensions when the shift and separation are scaled respectively by the single-particle plasmon wavelength maximum λ_0 and the particle size.[21] Accordingly, using the DDA method, we calculated the plasmon shift as a function of the interparticle separation for discs of different diameters at a constant aspect ratio $h/D \approx 0.3$ and medium dielectric constant $\epsilon_m = 1.0$. Figure 4a shows the plasmon shift versus the interparticle center-to-center distance for three different particle diameters, $D = 54$, 68, and 86 nm. With increasing particle size, the magnitude of the plasmon shift at a given interparticle distance increases (Figure 4a). In addition, the plasmon coupling exhibits a decay length, which increases with increasing nanodisc size (13.7, 15.5, and 17.5 nm, respectively). Figure 4b shows a plot of the fractional plasmon shift versus the ratio of the interparticle separation scaled by the nanodisc diameter for the three different particle sizes. It is seen that the decay trend becomes independent of the nanoparticle size on account of this scaling. On fitting with an exponential decay of the form $y = a \cdot e^{-x/\tau}$ (where $x = s/D$), the decay constant τ for this universal trend is estimated to be 0.23 ± 0.03, close to the experimental value $\tau = 0.18 \pm 0.02$ (Figure 4c). In essence, the plasmon

coupling decays over a length that is roughly 0.2 times the nanodisc diameter.

It is interesting to find that the decay constant estimated here closely matches the one observed by Gunnarson et al. ($\tau = 0.22$) in a system of nanodisc pairs of a different plasmonic metal, i.e., Ag.[27] The Ag system, however, exhibits larger magnitude of the plasmon shift (indicated by the parameter a of the fit), which can be attributed for by the well-known fact that the electromagnetic fields are stronger in the Ag system. In Au, the proximity of the plasmon resonance and the interband transition energies results in the damping of the plasmon resonance by interband electron excitations and hence in a reduction of the strength of the plasmonic field in comparison to the Ag system.[57] Regardless of this difference, the distance decay of the plasmon field itself appears to be independent of the nature of the metal.

We further investigate the simulated dependence of the distance decay of the plasmon shift on the medium dielectric constant. Figure 5a shows the calculated plasmon wavelength maximum versus the interparticle gap for three different values of the medium dielectric constant $\epsilon_m = 1.00$, 1.38, and 2.25, for constant nanodisc dimensions ($D = 86.5$ nm
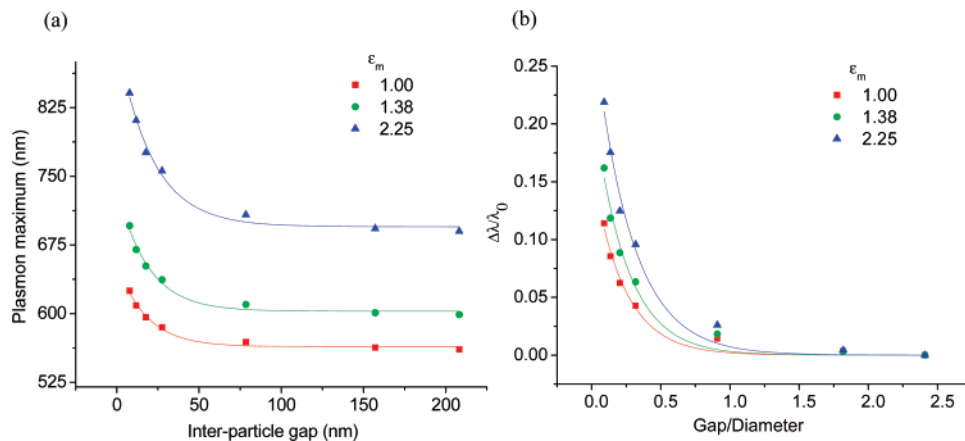
Figure 5. (a) Plot of the calculated plasmon maximum of the Au nanodisc pair system as a function of the interparticle distance for different values of the medium dielectric constant ϵ_m. The plot shows that the magnitude of the plasmon shift is higher for higher values of ϵ_m. (b) Plot of the calculated fractional shift versus the gap/diameter ratio for different ϵ_m. The data plots for different ϵ_m are fit to single-exponential decay $y = a \cdot e^{-x/\tau}$ (solid curves) with similar decay constant $\tau = 0.23 \pm 0.04$, 0.24 ± 0.03, and 0.27 ± 0.03 but increasing amplitude $a = 0.16 \pm 0.02$, 0.23 ± 0.02, and 0.29 ± 0.02 for $\epsilon_m = 1.00$, 1.38, and 2.25, respectively.
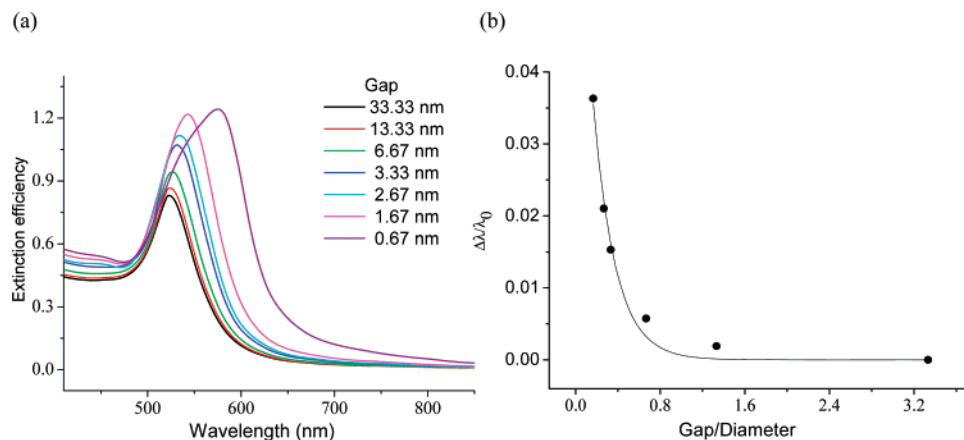

Figure 6. (a) DDA-simulated extinction efficiency spectra of 10 nm diameter Au nanosphere pair in water ($\epsilon_m = 1.77$) for varying interparticle separation gap for incident light polarization direction parallel to the interparticle axis. (b) Plot of fractional plasmon shift in Au nanosphere pair as a function of the gap/diameter ratio. The solid curve is a least-squares fit to an exponential decay function of the form $y = a \cdot e^{-x/\tau}$ where $a = 0.08 \pm 0.01$ and $\tau = 0.21 \pm 0.02$.

and $h = 25.5$ nm). It is well-established that the single-particle LSPR red-shifts with increasing medium dielectric constant ϵ_m, which we observe. However, we also observe that the extent of the plasmon shift (and hence the strength of the plasmon coupling) increases with an increase in the medium dielectric constant. This is counterintuitive to the well-known screening of electrostatic interactions in a higher dielectric constant medium. The plot of the fractional shift versus the gap/diameter ratio (Figure 5b) shows a decay rate, which is similar for the different values of ϵ_m while the amplitude increases with increasing dielectric constant ($\tau = 0.23$, 0.24, and 0.27; $a = 0.16$, 0.23, and 0.29 for $\epsilon_m = 1.00$, 1.38, and 2.25, respectively).

The nanoparticle shape also does not seem to have much influence on the decay behavior. We performed DDA calculations of the plasmon extinction efficiency of a pair of diameter 10 nm Au nanospheres, each represented by a $30 \times 30 \times 30$ cubic array of dipoles, corresponding to an interdipole spacing of 0.33 nm. The medium refractive index was 1.33 for water. The calculated spectra for the incident light polarization direction parallel to the interparticle axis

(Figure 6a) show that the plasmon band red-shifts with decreasing interparticle separation gap, similar to the case of the nanodisc pairs. The magnitude of the plasmon shift is much smaller in this case, as likely due to the smaller volume of these spheres as compared to the nanodiscs. However, the fractional plasmon shift versus the gap/diameter ratio (Figure 6b) follows a trend with a decay constant ($\tau = 0.21 \pm 0.02$) similar to that in the nanodisc system. At extremely small gap (i.e., 0.67 nm), where the particles are almost touching each other, a new band (possibly due to the quadrupolar mode) can be seen to emerge at shorter wavelengths. This data point is not included in the plot in Figure 6b. Experimentally, Reinhard et al.[43] have calibrated the distance dependence of the plasmon shift in a pair of 42 nm Au nanospheres, and from the fit to their data, we estimate their decay constant to be about 0.24. Simulations by Wei et al.[58] based on the T-matrix method and by Reinhard et al.[43] based on DDA also agree with these results, excluding particles that are nearly touching each other.

The universal scaling of the distance decay of plasmon coupling, demonstrated above, is also the likely reason for

Table 1. Experimental Interparticle Separation of Au Nanoparticle Pair Linked by DNA Spacers (Data from Reinhard et al.)[43] as Compared to the Interparticle Separation Calculated from the Observed Percentage Plasmon Shift (from the Experimental Fit of Reinhard et al.)[43] Using Our Plasmon Ruler Equation (eq 1)[a]

DNA spacer length[43] (base pairs)	observed $\Delta\lambda/\lambda_0$[43] (%)	experimental pair separation[43] (nm)	calculated separation from eq 1 (nm)
250	0.00	93	91
110	0.16	45	46
67	0.66	31	32
40	1.62	22	23
20	3.14	15	17
10	4.38	11	14

[a] Note that we have excluded from this analysis the data of Reinhard et al. for "pairs with zero separation". The experimental values of the pair separation in the third column were obtained as per the procedure of Reinhard et al., i.e., assuming a contour length of 0.34 nm per base pair and an additional distance of 8 nm to account for the thickness of the protein layer on the nanoparticles.[43]

the good agreement of our experimental and calculated decay constants despite the difference between the experimental parameters and those idealized in the simulations.

Plasmon Ruler Equation. We can take advantage of the universal scaling behavior to derive an empirical equation, which can be used to estimate the interparticle separation from an experimentally observed plasmon shift. This can serve as a useful calibration guide for the plasmon ruler designed to measure distances in biological systems.[42−44] The refractive index for proteins is estimated to be about 1.6.[43] We derive the "plasmon ruler equation"[59] for a Au particle pair in such a protein medium to be:

$$\frac{\Delta\lambda}{\lambda_0} \approx 0.18 \exp\left(\frac{-(s/D)}{0.23}\right) \qquad (1)$$

where $\Delta\lambda/\lambda_0$ is the fractional plasmon shift, s is the interparticle edge-to-edge separation, and D is the particle diameter. Reinhard et al.[43] recently obtained plasmon resonance spectra of pairs of 42 nm Au nanoparticles bound by ds-DNA spacers of known base pair lengths and therefore having defined interparticle separations (see Table 1). In their experiments, the dark-field microscopy technique was employed for obtaining plasmon spectra to ensure high spectral sensitivity and hence the observed $\Delta\lambda/\lambda_0$ is for the plasmon resonance scattering band. We use the plasmon ruler equation (eq 1) to calculate the interparticle separation s of a nanoparticle pair from the corresponding $\Delta\lambda/\lambda_0$ observed by Reinhard et al. (Table 1). Indeed, we get good agreement between our calculated values and the experimental interparticle separation, with reasonable deviations only at the smallest separations. It should also be noted that our calculated expression is for the light polarization direction along the interparticle axis, unlike the experiments in solution. But Reinhard et al. have already pointed out that experimental polarization effects have low significance for smaller nanoparticles (up to 40 nm size range); they become important for larger (87 nm) nanoparticles.[43]

Dipolar-Coupling Model. A simple model based on dipole−dipole interactions (Supporting Information) can provide us an intuitive picture of the distance decay of plasmon coupling in metal nanostructures. The dipolar coupling model, described by Kreibig and Vollmer,[1] has been found in the past to explain interparticle plasmon coupling effects with good qualitative agreement.[23,60] The dipolar near-field of a plasmonic particle is known to decay as the cube of the inverse distance,[30] as a result of which the plasmon coupling strength becomes a function of d^{-3}, a dependence which can be approximated very nearly to an exponential decay (Figure S1, Supporting Information). The polarization dependence can also be explained by the dipolar model on the basis of the orientation dependence of the near field.[50] The interesting size-scaling relationship can be understood as follows. The fractional plasmon shift ($\Delta\lambda/\lambda_0$) can be thought to reflect the strength of the interparticle electromagnetic coupling relative to the intraparticle plasmonic restoring potential.[24] While the interparticle dipolar coupling potential is known to decay with center-to-center distance as d^{-3},[30] the intraparticle restoring potential (reflected by the inverse of the dipole polarizability) is inversely proportional to the volume or D^3. As a result, $\Delta\lambda/\lambda_0$ becomes a function of $(d/D)^{-3}$ or $(s/D + 1)^{-3}$. Thus the dependence of the plasmon coupling strength on similar powers of separation s and diameter D allows the dimensional scaling of the function and hence the universality over particle pairs of varied dimensions. This functional dependence of fractional shift on $(s/D + 1)^{-3}$ also involves no contribution from the surrounding medium dielectric constant and the metal type. Moreover, the effect of shape is weak (Figure S2, Supporting Information). Thus the scaling behavior (indicated by the decay constant τ) is similar for different nanoparticle size, shape, metal type, or medium dielectric constant; these parameters only govern the magnitude of the fractional shift in the system (indicated by the amplitude a). For instance, the simple dipolar picture predicts that when the medium dielectric constant is changed from 1.00 to 2.25, the value of the amplitude nearly doubles without any significant effect on the decay constant (Figure S3, Supporting Information). This is similar to the observation from the DDA simulations (Figure 5b). The predicted effect of the medium dielectric constant on the plasmon shift deserves further experimental investigation. This can potentially be useful for the estimation of the local medium dielectric constant by plasmon resonance spectroscopy.

The quasistatic dipolar-coupling model, however, is qualitative because it does not take into account electromagnetic retardation effects as well as higher-order/multipolar interactions unlike the DDA method, where each particle is simulated by several thousand dipoles and retardation correction is included. As finite particle size and multipolar effects become increasingly important, deviations from the predictions of the dipolar model can be seen. Our observation is that the dipolar model underestimates the plasmon coupling strength at small interparticle gaps, in line with earlier analyses.[27,61] The dipolar model is clearly not valid for interactions between particles, which are nearly touching each

other.[27] In such a case, a complete treatment[61,62] involving all modes of interaction (dipolar, quadrupolar, ...) needs to be employed. We conjecture that the scaling may still be valid (only with a decay rate faster than that predicted by the purely dipolar model) when higher-order terms (e.g., quadrupoles) enter into the interaction at small interparticle separation. For instance, the quadrupolar interaction energy is proportional to the fifth power of the inverse distance, while the quadrupole polarizability is proportional to the fifth power of the particle dimensions.

Conclusion. In summary, our investigation of the plasmon resonances in Au nanodisc pairs shows that interparticle plasmon coupling strength for polarization along interparticle axis decays nearly exponentially with a decay length, which is roughly about 0.2 in units of the particle size for different nanoparticle size, shape, metal type, and medium dielectric constant. A dipolar-coupling model qualitatively explains that this behavior results from the interplay of two factors: the dependence of the single-particle polarizability on the cubic power of the particle dimension and the decay of the particle plasmon near-field as the cubic power of the inverse distance. The universal plasmon scaling behavior deduced in our work can be a useful guide for the design of nanostructured devices, which are based on interparticle plasmon coupling, especially the plasmon ruler.[43] The plasmon coupling strength has a softer dependence on the particle separation ($1/R^3$ within dipole approximation), thus providing a much longer interaction range as compared to FRET, which has a $1/R^6$ dependence.[45] Additionally, the particle size can be employed as a direct handle for increasing the ruler range, irrespective of the effect of nanoparticle shape, the metal type, or the medium dielectric constant. The quantification of the plasmon coupling decay behavior also allows us to derive a "plasmon ruler equation" that gives an estimate of the interparticle separation between spherical Au nanoparticles in a biological system from the fractional plasmon shift observed spectroscopically.

Supporting Information Available: DDA simulation procedure and details of the dipolar-coupling model (Figures S1−S3). This material is available free of charge via the Internet at http://pubs.acs.org.

References

(1) Kreibig, U.; Vollmer, M. *Optical Properties of Metal Clusters*; Springer: Berlin, 1995; Vol. 25.

(2) Kelly, K. L.; Coronado, E.; Zhao, L. L.; Schatz, G. C. *J. Phys. Chem. B* **2003**, *107*, 668−677.

(3) El-Sayed, M. A. *Acc. Chem. Res.* **2001**, *34*, 257−264.

(4) Link, S.; El-Sayed, M. A. *J. Phys. Chem. B* **1999**, *103*, 8410−8426.

(5) Bohren, C. F.; Huffman, D. R. *Absorption and Scattering of Light by Small Particles*; Wiley: New York, 1983.

(6) Hutter, E.; Fendler, J. H. *Adv. Mater.* **2004**, *16*, 1685−1706.

(7) Chen, C. K.; Heinz, T. F.; Ricard, D.; Shen, Y. R. *Phys. Rev. B* **1983**, *27*, 1965−1979.

(8) Schatz, G. C. *Acc. Chem. Res.* **1984**, *17*, 370−376.

(9) Jain, P. K.; Lee, K. S.; El-Sayed; I. H.; El-Sayed, M. A. *J. Phys. Chem. B* **2006**, *110*, 7238−7248.

(10) Sonnichsen, C.; Franzl, T.; Wilk, T.; von Plessen, G.; Feldmann, J.; Wilson, O.; Mulvaney, P. *Phys. Rev. Lett.* **2002**, *88*, 077402/1− 077402/4.

(11) Sokolov, K.; Follen, M.; Aaron, J.; Pavlova, I.; Malpica, A.; Lotan, R.; Richards-Kortum, R. *Cancer Res.* **2003**, *63*, 1999−2004.

(12) El-Sayed, I. H.; Huang, X.; El-Sayed, M. A. *Nano Lett.* **2005**, *5*, 829−834.

(13) Rosi, N. L.; Mirkin, C. A. *Chem. Rev.* **2005**, *105*, 1547−1562.

(14) Alivisatos, A. P. *Nature Biotechnol.* **2004**, *22*, 47−52.

(15) Haes, A. J.; Hall, W. P.; Chang, L.; Klein, W. L.; Van Duyne, R. P. *Nano Lett.* **2004**, *4*, 1029−1034.

(16) Huang, X.; El-Sayed, I. H.; Qian, W.; El-Sayed, M. A. *J. Am. Chem. Soc.* **2006**, *128*, 2115−2120.

(17) Hirsch, L. R.; Stafford, R. J.; Bankson, J. A.; Sershen, S. R.; Rivera, B.; Price, R. E.; Hazle, J. D.; Halas, N. J.; West, J. L. *Proc. Natl. Acad. Sci. U.S.A.* **2003**, *100*, 13549−13554.

(18) Huang, X.; Jain, P. K.; El-Sayed, I. H.; El-Sayed, M. A. *Photochem. Photobiol.* **2006**, *82*, 412−417.

(19) Jain, P. K.; El-Sayed, I. H.; El-Sayed, M. A. *Nano Today* **2007**, *2*, 18−29.

(20) Pileni, M. P. *J. Phys. Chem. B* **2001**, *105*, 3358−3371.

(21) Su, K. H.; Wei, Q.-H.; Zhang, X.; Mock, J. J.; Smith, D. R.; Schultz, S. *Nano Lett.* **2003**, *3*, 1087−1090.

(22) Jain, P. K.; Qian, W.; El-Sayed, M. A. *J. Phys. Chem. B* **2006**, *110*, 136−142.

(23) Rechberger, W.; Hohenau, A.; Leitner, A.; Krenn, J. R.; Lamprecht, B.; Aussenegg, F. R. *Opt. Commun.* **2003**, *220*, 137−141.

(24) Aizpurua, J.; Bryant, G. W.; Richter, L. J.; Garcia de Abajo, F. J.; Kelley, B. K.; Mallouk, T. *Phys. Rev. B* **2005**, *71*, 235420/1−235420/ 13.

(25) Seker, F.; Malenfant, P. R. L.; Larsen, M.; Alizadeh, A.; Conway, K.; Kulkarni, A. M.; Goddard, G.; Garaas, R. *Adv. Mater.* **2005**, *17*, 1941−1945.

(26) Lin, S.; Li, M.; Dujardin, E.; Girard, C.; Mann, S. *Adv. Mater.* **2005**, *17*, 2553−2559.

(27) Gunnarsson, L.; Rindzevicius, T.; Prikulis, J.; Kasemo, B.; Käll, M.; Zou, S.; Schatz, G. C. *J. Phys. Chem. B* **2005**, *109*, 1079−1087.

(28) Sweatlock, L. A.; Maier, S. A.; Atwater, H. A.; Penninkhof, J. J.; Polman, A. *Phys. Rev. B* **2005**, *71*, 235408/1−235408/7.

(29) Xiao, J. J.; Huang, J. P.; Yu, K. W. *Phys. Rev. B* **2005**, *71*, 045404/ 1−045404/8.

(30) Maier, S. A.; Brongersma, M. L.; Kik, P. G.; Atwater, H. A. *Phys. Rev. B* **2002**, *65*, 193408/1−193408/4.

(31) Kottmann, J. P.; Martin, O. J. F. *Opt. Express* **2001**, *8*, 655−663.

(32) Nie, S.; Emory, S. R. **1997**, *275*, 1102−1106.

(33) Michaels, A. M.; Jiang, J.; Brus, L. *J. Phys. Chem. B* **2000**, *104*, 11965−11971.

(34) Brongersma, M. L.; Hartman, J. W.; Atwater, H. A. *Phys. Rev. B* **2000**, *62*, R16356−R16359.

(35) Maier, S. A.; Brongersma, M. L.; Kik, P. G.; Meltzer, S.; Requicha, A. A. G.; Atwater, H. A. *Adv. Mater.* **2001**, *13*, 1501−1505.

(36) Maier, S. A.; Kik, P. G.; Atwater, H. A.; Meltzer, S.; Harel, E.; Koel, B. E.; Requicha, A. A. G. *Nat. Mater.* **2003**, *2*, 229−232.

(37) Krenn, J. R.; Salerno, M.; Felidj, N.; Lamprecht, B.; Schider, G.; Leitner, A.; Aussenegg, F. R.; Weeber, J. C.; Dereux, A.; Goudonnet, J. P. *J. Microsc.* **2001**, *202*, 122−128.

(38) Storhoff, J. J.; Elghanian, R.; Mucic, R. C.; Mirkin, C. A.; Letsinger, R. L. *J. Am. Chem. Soc.* **1998**, *120*, 1959.

(39) Storhoff, J. J.; Lazarides, A. A.; Mucic, R. C.; Mirkin, C. A.; Letsinger, R. L.; Schatz, G. C. *J. Am. Chem. Soc.* **2000**, *122*, 4640− 4650.

(40) Alivisatos, A. P.; Johnsson, K. P.; Peng, X.; Wilson, T. E.; Loweth, C. J.; Bruchez, M. P., Jr.; Schultz, P. G. *Nature* **1996**, *382*, 609.

(41) Storhoff, J. J.; Mirkin, C. A. *Chem. Rev.* **1999**, *99*, 1849−1862.

(42) Sonnichsen, C.; Reinhard, B. M.; Liphardt, J.; Alivisatos, A. P. *Nat. Biotechnol.* **2005**, *23*, 741−745.

(43) Reinhard, B. M.; Siu, M.; Agarwal, H.; Alivisatos, A. P.; Liphardt, J. *Nano Lett.* **2005**, *5*, 2246−2252.

(44) Reinhard, B.; Sheikholeslami, S.; Mastroianni, A.; Alivisatos, A. P.; Liphardt, J. *Proc. Natl. Acad. Sci. U.S.A.* **2007**, *104*, 2667−2672.

(45) Deniz, A. A.; Dahan, M.; Grunwell, J. R.; Ha, T.; Faulhaber, A. E.; Chemla, D. S.; Weiss, S.; Schultz, P. G. *Proc. Natl. Acad. Sci. U.S.A.* **2007**, *96*, 3670−3675.

(46) Lamprecht, B.; Schider, G.; Lechner, R. T.; Ditlbacher, H.; Krenn, J. R.; Leitner, A.; Aussenegg, F. R. *Phys. Rev. Lett.* **2000**, *84*, 4721−4724.

(47) Salerno, M.; Félidj, N.; Krenn, J. R.; Leitner, A.; Aussenegg, F. R.; Weeber, J. C. *Phys. Rev. B* **2001**, *63*, 165422/1−165422/6.

(48) Krenn, J. R.; Dereux, A.; Weeber, J. C.; Bourillot, E.; Lacroute, Y.; Goudonnet, J. P.; Schider, G.; Gotschy, W.; Leitner, A.; Aussenegg, F. R.; Girard, C. *Phys. Rev. Lett.* **1999**, *82*, 2590−2593.

(49) Tamaru, H.; Kuwata, H.; Miyazaki, H. T.; Miyano, K. *Appl. Phys. Lett.* **2002**, *80*, 1826−1828.

(50) Jain, P. K.; Eustis, S.; El-Sayed, M. A. *J. Phys. Chem. B* **2006**, *110*, 18243−18253.

(51) Krenn, J. R.; Schider, G.; Rechberger, W.; Lamprecht, B.; Leitner, A.; Aussenegg, F. R.; Weeber, J. C. *Appl. Phys. Lett.* **2000**, *77*, 3379−3381.

(52) Draine, B. T.; Flatau, P. J. *J. Opt. Soc. Am. A* **1994**, *11*, 1491−1499.

(53) Schatz, G. C. *THEOCHEM* **2001**, *573*, 73−80.

(54) Brioude, A.; Jiang, X. C.; Pileni, M. P. *J. Phys. Chem. B* **2005**, *109*, 13138−13142.

(55) Kelly, K. L.; Lazarides, A. A.; Schatz, G. C. *Comput. Scie. Eng.* **2001**, *3*, 67−73.

(56) Lamprecht, B.; Schider, G.; Lechner, R. T.; Ditlbacher, H.; Krenn, J. R.; Leitner, A.; Aussenegg, F. R. *Phys. Rev. Lett.* **2000**, *84*, 4721−4724.

(57) Pustovit, V. N.; Shahbazyan, T. V. *J. Opt. Soc. Am. A* **2006**, *23*, 1369−1374.

(58) Wei, Q.-H.; Su, K.-H.; Durant, S.; Zhang, X. *Nano. Lett.* **2004**, *4*, 1067−1071.

(59) This equation was estimated by the DDA simulation method with discrete dipole spacing of 1 nm and a nanosphere diameter of 40 nm. Similar to other analyses in this work, data points where the two particles nearly touch each other (indicated by emergence of an additional extinction band at shorter wavelengths) were excluded.

(60) Gluodenis, M.; Foss, C. A., Jr. *J. Phys. Chem. B* **2002**, *106*, 9484−9489.

(61) Nordlander, P.; Oubre, C.; Prodan, E.; Li, K.; Stockman, M. I. *Nano Lett.* **2004**, *4*, 899−903.

(62) Ruppin, R. *Phys. Rev. B* **1982**, *26*, 3440−3444.

NL071008A